Anchoring and droplet deformation in polymer dispersed liquid crystals: NMR study in an electric field

M. Ambrožič,[1] P. Formoso,[2] A. Golemme,[2] and S. Žumer[1,3]

[1]*Jožef Stefan Institute, Jamova 39, 1000 Ljubljana, Slovenia*
[2]*Chemistry Department, University of Calabria, Rende, Italy*
[3]*Physics Department, University of Ljubljana, Jadranska 19, 1000 Ljubljana, Slovenia*

We report a deuterium NMR study of nematic droplets, formed in a polymer dispersed liquid crystal (PDLC). An electric field with variable strength and direction orthogonal to the NMR magnetic field is applied to this liquid crystal, confined to submicrometer quasispherical cavities with planar surface anchoring. A broad transition from predominantly magnetic field aligned droplets to the electric field aligned limit is observed. The Frank-Oseen free energy with an additional surface energy term is used to find nematic director fields, free energies, and finally simulated NMR spectra of structures in different magnetic and electric fields. We are particularly interested in the influence of surface anchoring strength and nonspherical cavity shape on nematic structures and NMR spectra. Cavities are modeled by randomly oriented rotationally symmetric ellipsoids with a Gaussian distribution of elongations measuring droplet deformation. Simulated NMR spectra describe the experimental data very well and yield for the surface anchoring strength $(1 \pm 0.15) \times 10^{-3}$ J/m^2 and for the width of the deformation distribution $(15 \pm 1)\%$. The agreement with the scanning electron microscopy results indicates that deformations are the main cause of the random orientation of bipolar structures in these PDLC's. Using the known dielectric anisotropy of our nematic liquid crystal we found the electric field in the droplets to be 60% of the undisturbed electric field. [S1063-651X(97)10808-X]

I. INTRODUCTION

Nematic liquid crystals are attracting interest for fundamental and practical reasons [1]. Since the discovery of polymer dispersed liquid crystals (PDLC's) [2–5] numerous experimental and theoretical works have been performed on liquid crystals confined to spherical geometries [6–11]. PDLC's consist of small nearly uniform sized (down to submicrometer) droplets of a nematic liquid crystal in a solid polymer matrix. They are formed during the phase separation caused by a polymerization of organic monomers in a liquid-crystal–monomer mixture. PDLC's are attracting attention because of their application in scattering-based liquid-crystal displays and light shutters. The nematic structure, which is important for the performance of PDLC devices, is a result of the balancing of nematic elastic deformations, surface anchoring, and the influence of external fields. In spherical liquid-crystal droplets with twist elastic constant comparable to splay and bend elastic constants, the bipolar structure is stable for weak and strong planar anchoring [6].

Proton and deuterium nuclear magnetic resonance (NMR) spectroscopy is a powerful method for the investigation of nematic structures in submicrometer spherical droplets [12–15], but there were only few studies in the electric field. Holstein *et al.* used NMR to study molecular dynamics in thin polymeric liquid-crystal layers in external electric field [16]. To our knowledge, the simultaneous influence of two external fields, electric and magnetic, on nematic liquid-crystal structures in highly curved geometry has never been previously studied.

Although PDLC's are used for many applications, there are several unresolved questions about the liquid-crystal–polymer boundary interface. Here we will first discuss the strength of anchoring in submicrometer droplets, which is a difficult parameter to determine. Secondly, we will try to address the question of to what extent the orientation of the bipolar structure in droplets is determined by the shape of cavities, which are not exactly spherical, and to what extent the polymerization process induces a memory effect on the anchoring.

With such aims we decided to study nematic structures in submicrometer cavities of a PDLC in the presence of electric fields, using deuterium NMR spectroscopy. We investigated the transition in nematic director field, induced by increasing electric field strength, where the electric field is orthogonal to the static NMR magnetic field. The degenerate planar anchoring condition at the surface of cavities was assumed. We calculated nematic director fields, free energies, and NMR spectra of structures for different sets of physical parameters and we compared theoretical spectra with experimental results. From the analysis of the transition in the NMR spectra we were able to draw conclusions about surface anchoring and shapes of cavities in PDLC's.

In Sec. II we describe the experiment, and in Sec. III we lay the theoretical grounds for our phenomenological description of structures. In Sec. IV we discuss the results, compare experimental and theoretical NMR spectra, and estimate the values of some physical parameters. Finally, in Sec. V, we give a summary of the conclusions.

II. EXPERIMENT AND RESULTS

The samples with dispersed nematic droplets were made using polymerization-induced phase separation, involving an accurate mixing of the appropriate quantities of the various
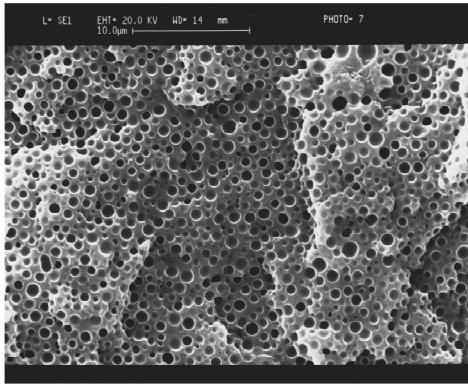
FIG. 1. SEM photograph of polymer dispersed liquid crystal without surfactant. The average radius of the droplets is 0.4 μm.
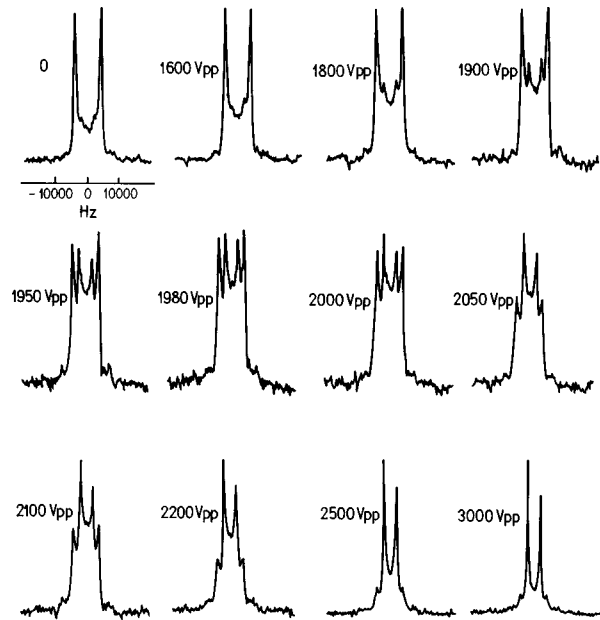

FIG. 2. The dependence of experimental deuterium NMR spectra on the magnitude of the applied electric field, perpendicular to the magnetic field. The peak-to-peak voltage is varied from 0 to 3000 V.

components, followed by a curing period at controlled temperature. The components used were resin, liquid crystal, and a deuterated probe. The anchoring is supposed to be degenerate planar, i.e., the preferred direction of the molecular long axis at the liquid-crystal-polymer network boundary is parallel to the surface. All directions in the preferred tangential plane are equivalent. The polymer matrix was formed using the two component epoxy glue Bostik (from Bostik S.p.A., Italy). Its component A is an equimolar mixture of Bisphenol A and epichlorohydrin, while the component B is a fatty polyamine curing agent. In all samples we used the nematic eutectic liquid-crystal mixture E7 (from BDH Chemicals, England). A small amount (3 wt %) of the deuterated probe hexamethylbenzene-d_{18} (HMB-d_{18}, from Cambridge Isotopes Labs, Woburn), with high melting point and 18 equivalent deuterium atoms, yielding one NMR signal, was dissolved in the liquid crystal. The epoxy components A and B were added to the nematic solution, thoroughly mixed and lightly centrifuged to remove air bubbles. The resulting homogeneous mixture was placed between two indium-tin oxide (ITO) coated conducting glasses, where the thickness of the cell 0.700 ± 0.005 mm was controlled using glass spacers at the corners of the cell. Samples sealed in the NMR measuring cell were cured at 60 °C for 48 h. After the NMR experiment was finished, the cells were broken and the averaged droplet size was measured using scanning electron microscopy (SEM). The droplet size was regulated by changing the relative amount of liquid crystal. Here we describe the case with the 34% weight concentration of E7, which yields an average droplet radius of 0.4 μm. The SEM photograph of a sample is shown in Fig. 1.

Deuterium NMR experiments were performed using a Bruker MSL 300 spectrometer, operating at 46.05 MHz in a 7-T magnetic field. The spectra with a typical width of about 10 kHz were recorded using a quadrupole echo technique ($\pi/2$-τ-$\pi/2$) with pulses of 9 μs separated by a 40-μs delay. The free induction decay (FID) for each spectrum was averaged 10 000 times to achieve a reasonable signal-to-noise ratio.

NMR experiments were performed while applying a 2-kHz ac voltage on the sample in the NMR coil, along a direction normal to the magnetic field. A special screening was used to reduce the noise increase to approximately twice the noise level observed without the electric field. The volt-

age of a wave form generator (Tectronix TM 503) was amplified by a home-built power amplifier. Its intensity, wave form, and frequency were constantly monitored. The peak-to-peak voltage difference was varied from 0 to 4000 V, which yielded an effective electric field strength between 0 and 2 V/μm.

Each spectrum is a superposition of two different and recognizable components: a more intense component from HMB-d_{18} dissolved in the liquid-crystalline droplets and a wider spectrum from solid HMB-d_{18} left within the polymeric matrix. Only the first component is of interest for our study. The solid HMB-d_{18} gives a slightly biaxial powder pattern ($\eta = 0,1$), about 32 kHz wide between the outer shoulders (Fig. 2).

Increasing the strength of the electric field, normal to the magnetic field, while keeping other physical parameters constant, NMR spectra reveal a continuous transition (droplet reorientation). In the case of nematic droplets of average radius 0.4 μm the transition is spread over the interval between about 1800 V (peak-to-peak) and 2500 V (peak-to-peak) (Fig. 2) corresponding to an effective electric field from 0.9 to 1.25 V/μm. The relative width of the transition with respect to the middle value of the field is about 30%.

Optical microscopy of a sample with larger (supramicrometer) cavities showed that the liquid-crystal structure in droplets was bipolar, which confirms a planar anchoring of liquid-crystal molecules at the droplet boundary.

III. THEORY AND RESULTS

Our nematic liquid-crystal structure is described in terms of a nematic director field $\mathbf{n}(\mathbf{r})$. We neglect the biaxiality and space variation of the scalar nematic-order parameter. First we calculate numerically nematic structures in various droplets with ideal spherical shape under the influence of

planar anchorings and electric and magnetic fields. Next we use these results for the approximate calculation of the director fields and NMR spectra of nonspherical droplets.

A. Spherical geometry

Spherical coordinates r, ϕ, and θ are used in the calculation of director fields and corresponding free energies in spherical geometry. The free energy of a nematic liquid crystal in a cavity with radius R is divided into a bulk elastic term, a magnetic and electric contribution, and a surface anchoring energy:

$$F = \int f_e dV + \int f_{E,B} dV + \int f_s dS. \tag{1}$$

The bulk Frank-Oseen free energy density is a sum of elastic deformation energy terms with different symmetries:

$$f_e = \tfrac{1}{2}[K_{11}(\boldsymbol{\nabla}\cdot\mathbf{n})^2 + K_{22}(\mathbf{n}\cdot\boldsymbol{\nabla}\times\mathbf{n})^2 + K_{33}(\mathbf{n}\times\boldsymbol{\nabla}\times\mathbf{n})^2$$
$$- K_{24}\boldsymbol{\nabla}\cdot(\mathbf{n}\times\boldsymbol{\nabla}\times\mathbf{n}+\mathbf{n}\boldsymbol{\nabla}\cdot\mathbf{n})], \tag{2}$$

where K_{11}, K_{22}, and K_{33} are splay, twist, and bend elastic constants, respectively, and K_{24} is the saddle-splay elastic constant. To make our discussion as simple as possible we omit the K_{13} (splay-bend) term and we use the approximation of equal bulk elastic constants: $K_{11}=K_{22}=K_{33}\equiv K$. The saddle-splay elastic constant is allowed to vary.

The field energy density is

$$f_{E,B} = -\frac{1}{2}\epsilon_0\Delta\chi_E(\mathbf{E}\cdot\mathbf{n})^2 - \frac{1}{2\mu_0}\Delta\chi_B(\mathbf{B}\cdot\mathbf{n})^2, \tag{3}$$

where $\Delta\chi_E$ and $\Delta\chi_B$ are the anisotropies of elastic and magnetic susceptibilities, respectively. In our case they are positive. In this paper we focus our attention on the case where the electric field is perpendicular to the NMR magnetic field.

Optical microscopy indicates planar anchoring. With the lack of additional information we assume that it is degenerate homogeneous (where all the directions in the surface plane are energetically equivalent), so that the surface free energy density can be described by a Rapini-Papoular form [17]:

$$f_s = \tfrac{1}{2}W_\theta\sin^2\theta'. \tag{4}$$

W_θ is the polar anchoring strength and θ' is the angle between the nematic director and its projection on the boundary plane.

It is convenient to introduce dimensionless (''reduced'') quantities for radius, elastic constants, fields, and anchoring strength:

$$\rho = \frac{r}{R}, \tag{5}$$

$$\mathcal{K}_{24} = K_{24}/K, \tag{6}$$

$$\mathcal{W}_\theta = R W_\theta/K, \tag{7}$$

$$\mathcal{E} = ER(\epsilon_0\Delta\chi_E/K)^{1/2}, \tag{8}$$

$$\mathcal{B} = BR[\Delta\chi_B/(\mu_0 K)]^{1/2}, \tag{9}$$

$$\mathcal{F} = \frac{F}{KR}. \tag{10}$$

We take the bulk elastic constants for E7 from the literature [18]: $K_{11}=11.7\times10^{-12}$ J/m, $K_{22}=8.8\times10^{-12}$ J/m, and $K_{33}=19.5\times10^{-12}$ J/m and we set the effective elastic constant to their average value: $K=13.3\times10^{-12}$ J/m. The magnetic susceptibility anisotropy of E7 is $\Delta\chi_B=1.37\times10^{-6}$ [19], thus we obtain the magnitude of the dimensionless magnetic field: $\mathcal{B}\approx0.8$. In the present calculations the magnetic field is kept at this value, while the electric field is varied.

We express the nematic director in terms of two angles: nematic polar angle Ω and nematic azimuthal angle Ψ. Both are functions of spherical coordinates: $\Omega=\Omega(\rho,\theta,\phi)$ and $\Psi=\Psi(\rho,\theta,\phi)$. The form of the nematic director in Cartesian coordinates is $\mathbf{n}=(\sin\Omega\cos\Psi,\sin\Omega\sin\Psi,\cos\Omega)$. The polar angle Ω is the angle between the nematic director and the z axis, while the azimuthal angle Ψ is the angle between the projection of the nematic director on the (x,y) plane and the x axis.

Minimizing the free energy with respect to Ω and Ψ yields a coupled set of two partial differential equations, which is solved by a relaxation method. A more detailed description of this procedure will be given elsewhere. In the presence of a single field, say the magnetic field, the possible solution of the minimization problem is a bipolar structure [6,20] with cylindrical symmetry around the field direction. The bipolar structure with the symmetry axis parallel to the z axis is thus defined by the nematic polar angle $\Omega(\rho,\theta)$, while for the nematic azimuthal angle we have $\Psi=\phi$.

The resulting free energy and NMR spectra are calculated by performing numerical integration. We take the natural width of the NMR lines 0.1 in units of frequency, where the two peaks of the bulk nematic, parallel to the NMR magnetic field, are at the frequencies ±1. This choice of the theoretical NMR linewidth is based on the experimental NMR spectrum of a bulk sample where peaks at frequencies ±5 kHz have a 0.5-kHz width at half height. The calculated spectra are mostly normalized to give a unit area under the curves.

We have found that varying the saddle-splay elastic constant $\mathcal{K}_{24}$ from 0 to 2 has a negligible influence on our structures. Thus $\mathcal{K}_{24}$ is unimportant in our further discussion. We have not made any calculations for larger values of saddle-splay elastic constant since such cases are not reported in the literature.

In the case of dimensionless anchoring strengths of the order 5 or more, the fields (electric and magnetic) of the order 1 have no influence on the nematic director field, other than turning the bipolar symmetry axis. On the other hand, for smaller anchoring strengths the nematic director field is almost aligned (weak anchoring limit of a bipolar structure), and the direction of the nematic field is again determined by the field. Thus the symmetric bipolar structure is an excellent approximation. Figure 3 shows equilibrium nematic director fields in the central cross-section plane of droplets for different values of anchoring strength. The dependence of the free energy on anchoring strength is shown in Fig. 4.
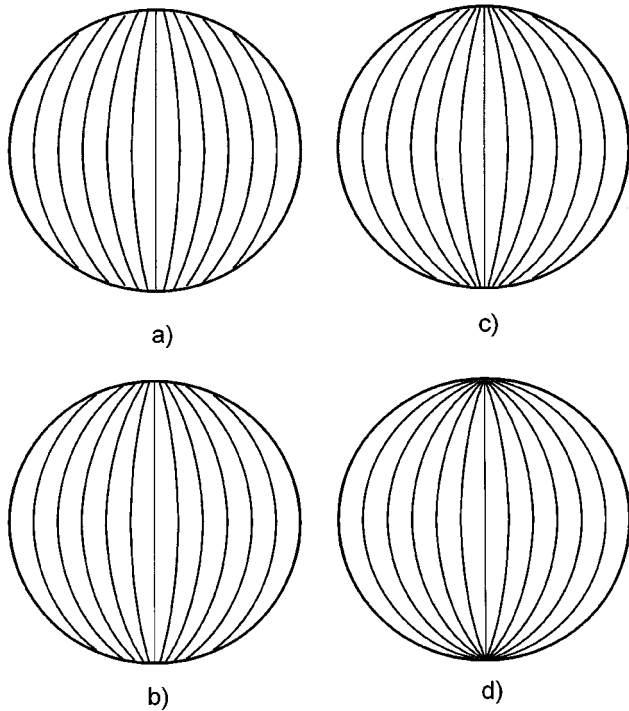
FIG. 3. Nematic zero field bipolar structures for different values of dimensionless anchoring strength: $\mathcal{W}_\theta = 10$ (a), 20 (b), 30 (c), and ∞ (d).

The direction of the bipolar axis for given magnitudes and directions of the fields **E** and **B** is the same as the direction of the nematic director would be in bulk samples. If the angle between the fields is 90°, the bipolar axis is parallel to the stronger field. Keeping the magnetic field constant, while increasing the electric field, there is a discontinuous jump in the nematic director field and NMR spectra at the point $\mathcal{E} = \mathcal{B}$. The bipolar axis turns towards the electric field direction at the transition point and the line splitting in NMR spectra reduces to half the value. In the cases where the angle between the electric and magnetic field is different from 90°, the orientation of the bipolar axis is again equal to the orientation of the homogeneous nematic director in a corresponding bulk sample.

B. Nonspherical geometry

Deformed droplets are modeled by rotationally symmetric ellipsoids (oblate or elongated). We assume constant volume of all droplets, thus half-axes measured in units of radius of nondeformed spheres are selected by the condition $a^2 c = 1$. To describe the deformation we assume a uniform distribution of the directions of the ellipsoid symmetry axis c axis in space. The value of the symmetry half-axis can be written as $c = 1 + \epsilon$, where ϵ is degree of deformation. Moreover, we assume a Gaussian distribution of deformations:

$$P(\epsilon) = \frac{1}{\sigma \sqrt{2\pi}} e^{-\epsilon^2/2\sigma^2}, \qquad (11)$$

where σ characterizes its width. In our calculations we take σ to be at most 0.2, so that there is always a negligible probability for the meaningless range $\epsilon < -1$.
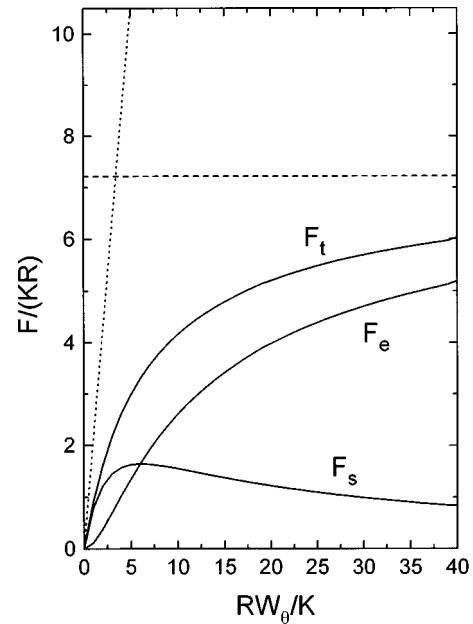

FIG. 4. Dimensionless elastic ($\mathcal{F}_e$), surface ($\mathcal{F}_s$), and total free energy ($\mathcal{F}_t = \mathcal{F}_e + \mathcal{F}_s$) of the nematic bipolar structure as functions of dimensionless anchoring strength $\mathcal{W}_\theta$ for spherical droplets in zero fields. The dashed line indicates a strong anchoring limit of the free energy. The dotted line indicates the free energy of aligned nematic director field. The total free energy is proportional to the effective anchoring strength [Eq. (14)].

Instead of solving minimization equations for deformed droplets [21,22] we will be able to use an approximate description. We first consider a single droplet and evaluate the influence of the droplet deformation on the nematic director field for the chosen ϵ and c direction. The deformation has two effects on nematic director: (i) it changes slightly the nematic director field without turning the bipolar axis (for instance, if $\epsilon > 0$, c is parallel to **B**, and **E** $=0$). (ii) It tends to turn the nematic bipolar axis, competing with magnetic and electric field.

Choosing a simple example with strong anchoring and relatively strong droplet deformation ($\sigma = 0.2$) we show that the influence of the mechanism (i) on NMR spectra is negligible in comparision with the mechanism (ii). We consider the case where the c axis is parallel to the magnetic field with $\mathcal{B} = 1$. We transform the nematic director **n** to the one in the deformed droplet **n**′ using the following transformation:

$$n'_x(ax, ay, cz) = a n_x(x, y, z)/D, \qquad (12a)$$

$$n'_y(ax, ay, cz) = a n_y(x, y, z)/D, \qquad (12b)$$

$$n'_z(ax, ay, cz) = c n_z(x, y, z)/D, \qquad (12c)$$

where $D = \sqrt{a^2(n_x{}^2 + n_y{}^2) + c^2 n_z{}^2}$ is a normalization parameter. The above transformation preserves the tangential molecular orientation at the droplet boundary. After transforming **n** we numerically calculate NMR spectra for ellipsoidal droplets. Adding together spectra for different values of ϵ, with the weights according to Eq. (11) and the assumption of a random distribution of c axes, we get a resulting NMR

$\mathcal{W}_\theta$	$\mathcal{W}_{\text{eff}}$	$\mathcal{P}$ ($\epsilon = 0.15$)
10	2.0	0.85
20	2.5	0.95
30	2.7	0.99
40	2.9	1.02
50	2.95	1.03
∞	3.5	1.12

spectrum. The difference between this spectrum and the spectrum from undeformed spherical droplet is found to be negligible.

Recognizing that the influence of the droplet deformation on the nematic director field is similar to the effect of another field we introduce a deformation field **P** as an approximate description of this effect. To achieve this we estimate the dependence of the total droplet free energy on the angle ω between the bipolar axis and the c axis (with no electric and magnetic field). First we calculate the free energy of the aligned nematic director field as a function of $\mathcal{W}_\theta$, ϵ, and ω. The aligned structure is not the one with minimal free energy, but the calculation of its free energy gives us insight into the influence of the droplet deformation on the nematic director field direction. The free energy of such an aligned director field consists only of the surface contribution. Expanding the surface free energy density in powers of ϵ and keeping only constant and linear terms we obtain an approximate analytical expression for the dimensionless surface free energy:

$$\mathcal{F}_s = \frac{2\pi\mathcal{W}_\theta}{3}\left(1 + \frac{4\epsilon}{5}(1 - 3\cos^2\omega)\right). \quad (13)$$

The first term corresponds to the surface free energy of the aligned nematic director field in a spherical droplet. The energy dependence on the angle ω can be seen in the third term with $\cos^2\omega$, which has the same form as the electric or magnetic free energy of an aligned nematic director field. To estimate the free energy of a deformed bipolar droplet, we keep the form (13), except that we correct the expression by introducing an ''effective'' anchoring strength $\mathcal{W}_{\text{eff}}$ instead of real anchoring $\mathcal{W}_\theta$. To find $\mathcal{W}_{\text{eff}}$ we take a particular anchoring strength $\mathcal{W}_\theta$ and calculate the equilibrium free energy $\mathcal{F}_{\text{eq}}$ of the bipolar structure in a spherical droplet. The value of the anchoring strength $\mathcal{W}_{\text{eff}}$ is defined so that it yields the same free energy in the case of aligned nematic director (Fig. 4). Thus $\mathcal{W}_{\text{eff}}$ is given by the equation

$$\mathcal{F}_{\text{eq}} = 2\pi\mathcal{W}_{\text{eff}}/3. \quad (14)$$

The effective anchoring strength is thus proportional to the total free energy of a nematic bipolar structure, which is shown in Fig. 4. Some values of the anchoring strength and of the corresponding effective anchoring strengths are shown in Table I. In addition, we suppose that for small deformation of droplets (small ϵ) Eq. (13) with the substitution $\mathcal{W}_\theta \rightarrow \mathcal{W}_{\text{eff}}$ satisfactorily describes deformed droplets. To
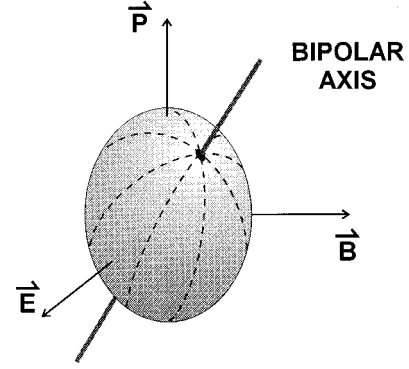

FIG. 5. An example of different directions of the fields **E**, **B**, and **P**, and the equilibrium direction of the bipolar axis. The director field on the droplet surface for strong anchoring is sketched by dashed lines.

study the orientation of the bipolar axis due to the deformation of the droplet we need only the third term in Eq. (13). The deformation field is parallel to the ellipsoidal c axis and its dimensionless magnitude is given by

$$\mathcal{P} = \sqrt{\tfrac{12}{5}\mathcal{W}_{\text{eff}}}|\epsilon|. \quad (15)$$

Some values of the effective anchoring strength and of the corresponding deformation field for $\epsilon = 0.15$ for different values of polar anchoring strength are listed in Table I. We see that even for infinite anchoring strength and relatively strong deformation the deformation field is relatively low (of the order 1).

In summary, we have three fields **E**, **B**, and **P**, which tend to reorient the bipolar axis (Fig. 5), but nevertheless they are two weak to significantly modify the bipolar nematic structure, which is predominantly determined entirely by the anchoring strength. This enables us to approximately determine the orientation $\mathbf{e}_{BP}$ of the bipolar axis by a minimization of a simple free energy of the fields:

$$\mathcal{F} = \tfrac{1}{2}[-\mathcal{E}^2(\mathbf{e}_E \cdot \mathbf{e}_{BP})^2 - \mathcal{B}^2(\mathbf{e}_B \cdot \mathbf{e}_{BP})^2 \pm \mathcal{P}^2(\mathbf{e}_P \cdot \mathbf{e}_{BP})^2], \quad (16)$$

where $\mathbf{e}_E$, $\mathbf{e}_B$, and $\mathbf{e}_P$ are directions of electric, magnetic, and deformation field, respectively.

The free energy of the $\mathcal{P}$ field contribution can have, in contrast to the electric and magnetic energy, either sign, because it is proportional to ϵ. This can be easily understood: if $\epsilon > 0$, the ellipsoid is elongated—the surface of such an ellipsoid is on the average more parallel to the c axis than to any other direction. Therefore the nematic director tends to orient parallel to the c axis. For $\epsilon < 0$ the opposite is true—the ellipsoid is oblate, so the nematic director tends to orient perpendicular to the c axis. After the determination of the equilibrium bipolar axis direction with respect to the magnetic field we can calculate the expected NMR spectrum. We take the same natural width of NMR lines and normalization condition as in the case of spherical geometry.
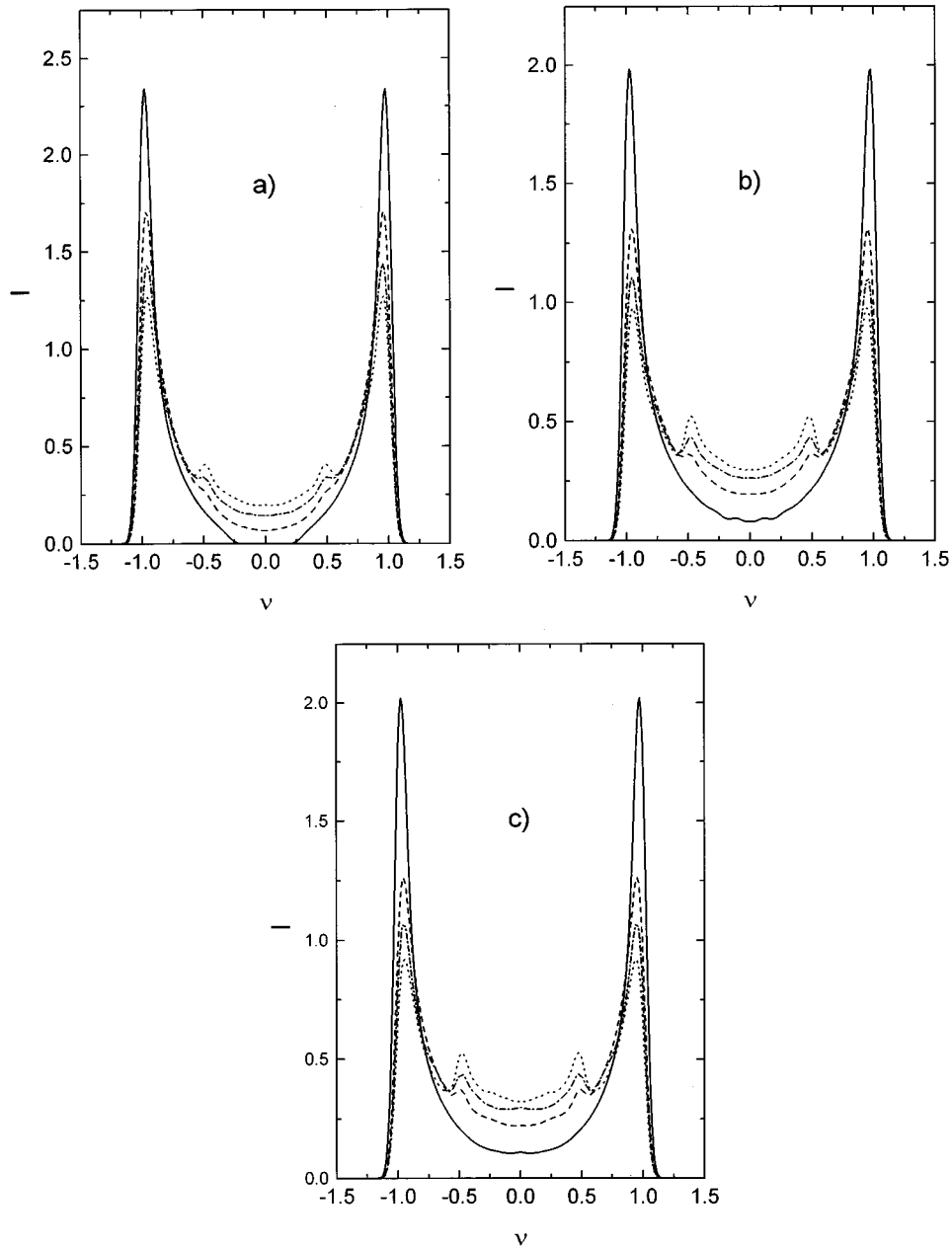
FIG. 6. The influence of the anchoring strength and deformation distribution width on calculated spectra for zero electric field. The bipolar axis is parallel to the magnetic NMR field of strength $\mathcal{B}=0.8$. The values of $\mathcal{W}_\theta$ are 10 (a), 30 (b), and 50 (c), while the values of σ are 0 (solid lines), 0.1 (dashed lines), 0.15 (dashed-dotted lines), and 0.2 (dotted lines). Both frequency ν and intensity I are dimensionless variables. I is normalized to give the unit area under the curves.

Keeping the electric and magnetic fields constant, we average spectra over different ϵ, using Gaussian weights (11) and over different directions of the c axis (equal weights). The induced transition in the shape of NMR spectrum occurring when $\mathcal{E}$ passes the point $\mathcal{E}=\mathcal{B}$ is studied depending on the distribution width σ. Dimensionless anchoring strength and droplet deformation distribution are varied to give the best agreement between experimental and theoretical results. The frequency ν used in calculated spectra (Figs. 6 and 7) is normalized with respect to the frequency of the peaks in bulk nematic spectrum of a sample with nematic director parallel to the NMR magnetic field.

IV. COMPARISON BETWEEN EXPERIMENTAL AND THEORETICAL NMR SPECTRA

Experimental spectra reveal a continuous transition at $\mathcal{E}\approx\mathcal{B}$ for perpendicular fields, in contradiction to the discontinuous theoretical transition for spherical droplets. According to the above discussion we suggest that the possible mechanism for finite transition width is due to the distribution of nonideal spherical shapes of nematic droplets in the polymer matrix. We estimate the value of anchoring strength and deformation distribution width by comparing the calculated and experimental spectra for $\mathbf{E}=0$. We subtract the background from the experimental spectra to achieve accu-
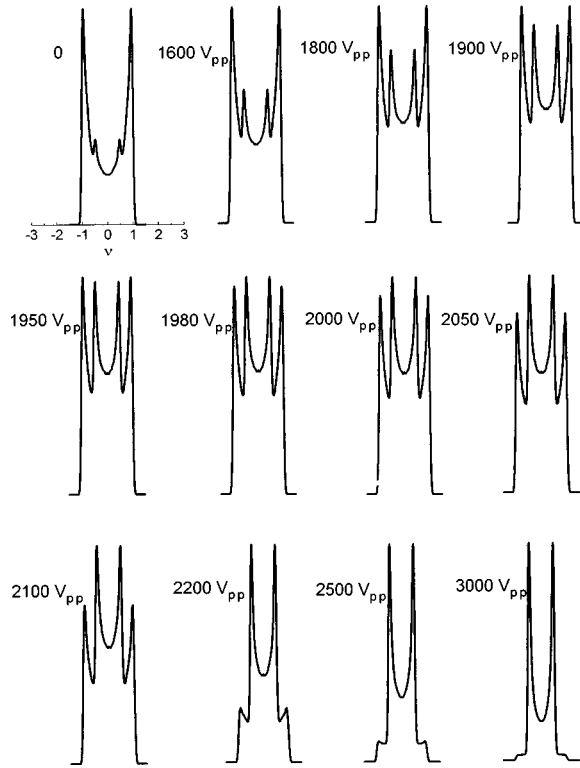
FIG. 7. The dependence of calculated NMR spectra on the magnitude of the applied electric field, perpendicular to the magnetic field, if a distribution of the deformations of spherical droplets is taken into account; $\mathcal{W}_\theta = 30$, $\sigma = 0.15$. Both variables frequency and intensity are dimensionless. The intensity is normalized to give the same height of higher lines in all spectra. This kind of normalization was chosen to enable direct comparison to the experimental spectra in Fig. 2.

rate comparison. The presence of a significant central part in the spectra indicates that $\mathcal{W}_\theta$ and σ are rather large. The experimental spectrum has four lines. The distance between the inner lines is half the distance between the outer lines, which are much higher then the inner lines for zero electric field (Fig. 2). To compare experimental and theoretical spectra we focus our attention on the following parameters: $\mathcal{R}_1$: the ratio between the width of the lines to the separation between the lines; $\mathcal{R}_2$: the ratio between the height of the central part of spectra to the height of the lines; $\mathcal{R}_3$: the ratio between the height of inner lines to the height of outer lines; $\mathcal{R}_4$: the ratio between the separation of inner lines to the separation of outer lines.

The width of the theoretical lines is mainly governed by the natural width and the deformation distribution width and to a smaller extent by the anchoring strength (Fig. 6). The experimental NMR spectrum in droplets reveals a three times larger line width in comparison to the bulk value. The theoretical ratios $\mathcal{R}_2$ and $\mathcal{R}_3$ strongly depend on anchoring strength and deformation distribution width, while the ratio $\mathcal{R}_4$ varies only slightly ($R_4 \approx 0.5$ as in the experiment) (Fig. 6). The best agreement between the experiment and theory is obtained for $\mathcal{W}_\theta = 30 \pm 5$ [the corresponding anchoring strength is about $(1 \pm 0.15) \times 10^{-3}$ J/m^2] and $\sigma = 0.15 \pm 0.01$. Table II shows a good agreement between experimental and theoretical parameters of the NMR spectra for $\mathcal{W}_\theta = 30$ and $\sigma = 0.15$.

TABLE II. The experimental and theoretical ($\mathcal{W}_\theta = 30$, $\sigma = 0.15$) NMR spectral parameters.

Parameter	Experiment	Theory
$\mathcal{R}_1$	0.15	0.145
$\mathcal{R}_2$	0.2	0.24
$\mathcal{R}_3$	0.3	0.39
$\mathcal{R}_4$	0.50	0.51

We estimate the deformation distribution using the SEM picture of the sample. The cross section of an ellipsoid with a plane is an ellipse. Spatial distribution of ellipsoids with variable c axis length and direction involves a planar distribution of ellipses in the cutoff plane. Measuring the ratio between the long and short axis lengths of the ellipses in the SEM photograph reveals a Gaussian distribution of deformations with the width $\sigma = 0.15 \pm 0.02$. This is in very good agreement with the theoretical prediction. Good agreement between experimental and calculated spectra reveals that the tangential alignment of liquid-crystal molecules at the droplet boundary is mainly governed by planar surface anchoring, rather than by other mechanisms, such as memory effects induced during the polymerization process [23].

Next we compare the experimental and theoretical spectra (taking $\mathcal{W}_\theta = 30$ and $\sigma = 0.15$) for nonzero electric field. There is a good agreement in the shapes of spectra and also in the relative electric field transition width (Figs. 2 and 7). The electric field induced transition of the spectra supports the estimation of the values of anchoring strength and deformation width, obtained from the zero field spectrum. By comparing experimental and theoretical spectra we can also calculate the value of the unknown dielectric anisotropy: $\Delta \chi_E \approx 5$. The value of $\Delta \chi_E$ from the literature is 13.8 [19], nearly three times larger. This discrepancy can be explained as follows. The dielectric constant of the liquid crystal E7 is large (19 and 5.2 for the long and short molecular axis direction, respectively) and is expected to differ considerably from the polymer matrix dielectric constant. Other electric effects may also appear, such as conductivity of the polymer matrix. These effects result in a different (and also inhomogeneous) electric field in the nematic droplets in comparison to the outside field [22]. We made an estimation of the flexoelectric contribution to the free energy. Using the typical value for flexoelectric coefficients ($e_{11} = e_{33} \approx 10^{-11}$ A s/m), we found the flexoelectric field energy to be about five times smaller than the electric contribution in Eq. (3) in the case $E = 2$ V/μm. Using the value $\Delta_{\chi E} = 13.8$ we obtain the average electric field in the droplets from Eq. (8): $E = 60\% E_0$, where E_0 is undistorted electric field in the NMR cell without the sample. Measurement of the electric field induced transition in NMR spectra is therefore a useful tool to estimate the actual electric field in nematic droplets inside the polymer matrix.

V. CONCLUSION

We investigated the deformation of liquid-crystal droplets in a polymer matrix by studying NMR spectra of a PDLC sample. In addition to the fixed NMR magnetic field, a variable perpendicular electric field was applied. The droplet de-

formation results in a broad continuous transition in NMR spectra upon increasing the electric field. The value of the planar anchoring strength was estimated to be $W_\theta = (1 \pm 0.15) \times 10^{-3}$ J/m^2. The distribution width of droplet deformation was found to be $\sigma = (15 \pm 1)\%$. Using the experimental value of dielectric anisotropy we estimated the average electric field in the droplets; It is 60% of the value of undistorted electric field in the NMR cell. Good agreement between experimental and theoretical NMR spectra supports our model, where the finite width of the NMR transition is caused by deformation of spherical droplet shapes into randomly oriented rotational ellipsoids.

ACKNOWLEDGMENTS

[1] See, for instance, *Handbook of Liquid Crystal Research*, edited by P. J. Collins and J. S. Patel (Oxford University Press, New York, 1997), and the relevant references therein.

[2] J. W. Doane, N. A. Vaz, B. G. Wu, and S. Žumer, Appl. Phys. Lett. **48**, 269 (1986).

[3] J. Fergason, SID (Soc. Info. Display), Int. Symp. Dig. Tech. Papers **16**, 68 (1985).

[4] J. W. Doane, A. Golemme, J. L. West, J. B. Whitehead, and B. G. Wu, Mol. Cryst. Liq. Cryst. **65**, 511 (1988).

[5] P. S. Drzaic, *Liquid Crystal Dispersions* (World Scientific, Singapore, 1995).

[6] R. D. Williams, J. Phys. A **19**, 3211 (1986).

[7] O. D. Lavrentovich and E. M. Terentev, Zh. Eksp. Teor. Fiz. **91**, 2084 (1986) [Sov. Phys. JETP **64**, 1237 (1986)].

[8] J. H. Erdmann, S. Žumer, and J. W. Doane, Phys. Rev. Lett. **64**, 1907 (1990).

[9] P. Drzaic, Mol. Cryst. Liq. Cryst. **154**, 289 (1988).

[10] S. Kralj and S. Žumer, Phys. Rev. A **45**, 2461 (1992).

[11] F. Xu, H. S. Kitzerow, and P. P. Crooker, Phys. Rev. E **49**, 3061 (1994).

[12] E. Berggren, C. Zannoni, C. Chiccoli, P. Pasini, and F. Semeria, Phys. Rev. E **49**, 2929 (1994).

[13] A. Golemme, S. Žumer, J. W. Doane, and M. E. Neubert, Phys. Rev. A **37**, 559 (1988).

[14] A. Golemme, S. Žumer, D. W. Allender, and J. W. Doane, Phys. Rev. Lett. **61**, 2937 (1988).

[15] M. Vilfan, V. Rutar, S. Žumer, G. Lahajnar, R. Blinc, J. W. Doane, and A. Golemme, J. Chem. Phys. **89**, 597 (1988).

[16] P. Holstein, D. Geschke, J. Rauchfuss, and M. Winkler (unpublished).

[17] B. Jerome, Rep. Prog. Phys. **54**, 391 (1991).

[18] E. P. Raynes, R. J. A. Tough, and K. A. Davies, Mol. Cryst. Liq. Cryst. Lett. **56**, 63 (1979).

[19] S T. Wu, W. H. Smith, and A. U. Lackner, Mol. Cryst. Liq. Cryst. **140**, 83 (1986).

[20] E. Dubois-Violette and O. Parodi, J. Phys. C **4**, 57 (1969).

[21] A. Kilian, Liq. Cryst. **14**, 1189 (1993).

[22] T. Onozawa, Liq. Cryst. **17**, 635 (1994).

[23] O. A. Aphonin, Proc. SPIE **2731**, 168 (1996).